Langerhans Cells Directly Interact with Resident T Cells in the Human Epidermis

Tomonori Oka[1,2], Tatsuya Hasegawa[1,2,3], Truelian Lee[1,2], Valeria S. Oliver-Garcia[1,2], Mahsa Mortaja[1,2], Marjan Azin[1,2], Satoshi Horiba[1,2,3], Sabrina S. Smith[1,2], Sara Khattab[1], Kathryn E. Trerice[1,2], Steven T. Chen[4], Yevgeniy R. Semenov[4,5] and Shadmehr Demehri[1,2,4]

Adult human skin contains nearly twice as many T cells as the peripheral blood, which include tissue-resident memory T cells. However, the precise mechanisms maintaining tissue-resident memory T cells in the healthy skin remain unclear. Using normal human skin samples, we find that Langerhans cells (LCs) contact T cells in the epidermis of the elderly. LCs with high HLA-II, CD86, and PD-L2 expression directly contacted PD-1$^+$ tissue-resident memory T cells and CTLA-4$^+$ regulatory T cells in the epidermis, indicating an axis of peripheral tolerance in a steady state. Environmental insults, UVB radiation, and hapten downregulated HLA-II and CD86 on LCs in the epidermis, suggesting that disruption of LC−T cell tolerogenic axis contributes to skin inflammation. Interestingly, immune checkpoint blockade therapy was associated with decreased epidermal LC−T cell contact in the normal skin of patients with cancer affected by cutaneous immune-related adverse events. Collectively, our findings indicate that LCs may contribute to T cell tolerance in the epidermis.

Keywords: Immune checkpoint, Langerhans cell, Peripheral tolerance, Regulatory T cell, Tissue-resident memory T cell

JID Innovations (2025);**5:**100324 doi:10.1016/j.xjidi.2024.100324

INTRODUCTION

The human skin harbors a large pool of T cells, with the majority being effector memory T cells (Clark et al, 2006). Tissue-resident memory T (TRM) cells are a noncirculating memory T-cell subset that populates peripheral tissues and provides local surveillance against pathogens and cancer (Gebhardt et al, 2018; Tokura et al, 2020). However, excessive activation of skin TRM cells can lead to pathological conditions, including fixed drug eruption, psoriasis, vitiligo, and alopecia (Ryan et al, 2021). Tissues maintain immune homeostasis through a delicate equilibrium between T cell activation against pathogens and the suppression of an exuberant T cell response targeting self-antigens and commensals. Understanding the precise mechanisms controlling TRM cell activity in peripheral organs is critical to promoting health and preventing inflammatory diseases.

Langerhans cells (LCs) are a unique population of tissue-resident antigen-presenting cells (APCs) residing in the epidermis. Considering that the skin is the outermost interface between the body and the external environment, LCs are strategically placed as immune sentinels and serve as the first line of immunological defense. Studies have delineated the dual roles of LCs as both immunostimulatory and immunoregulatory, dependent on the context and experimental model (Lutz et al, 2010; Stoitzner, 2010; Zhou et al, 2022). However, the precise function of LCs under normal conditions in human skin and their potential interactions with TRM cells residing in the epidermis remains unclear.

In this study, we investigated the interaction between LCs and TRM cells in the human epidermis. LCs directly contacted T cells in the epidermis of normal skin, which was increased with aging. LCs that contacted T cells were HLA-II^{high}, CD86$^+$, and PD-L2$^+$. In turn, T cells that contacted LCs in the epidermis expressed CTLA-4, Foxp3, and PD-1. These findings suggest that LC−T cell interaction in the epidermis may promote T-cell tolerance. Common environmental insults, UVB radiation and contact allergen, and immune checkpoint blockade (ICB) therapy disrupted the LC−T cell tolerogenic axis in the skin. Together, our findings indicate a potential tolerogenic role for direct LC−T cell interaction in the epidermis that may contribute to skin homeostasis.

RESULTS

LCs and T cells directly interact in the human epidermis

Given the continuous exposure of human skin to environmental stimuli leading to the accumulation of T cells in the skin with aging (Hasegawa et al, 2023), we explored the regulation of T cells residing in healthy human skin.

[1]*Center for Cancer Immunology is a part of Krantz Family Center for Cancer Research, Massachusetts General Hospital and Harvard Medical School, Boston, Massachusetts, USA;* [2]*Cutaneous Biology Research Center, Department of Dermatology, Massachusetts General Hospital and Harvard Medical School, Boston, Massachusetts, USA;* [3]*Shiseido Global Innovation Center, Yokohama, Japan;* [4]*Department of Dermatology, Massachusetts General Hospital and Harvard Medical School, Boston, Massachusetts, USA; and* [5]*Laboratory of Systems Pharmacology, Harvard Program in Therapeutic Science, Harvard Medical School, Boston, USA*

Correspondence: Shadmehr Demehri, Department of Dermatology, Massachusetts General Hospital, Building 149 13th Street, 3rd floor, Charlestown, Massachusetts 02129, USA. E-mail: sdemehri1@mgh.harvard.edu

Abbreviations: APC, antigen-presenting cell; cirAE, cutaneous immune-related adverse event; DNFB, 2,4-dinitrofluorobenzene; ICB, immune checkpoint blockade; LC, Langerhans cell; Treg, regulatory T cell; TRM, tissue-resident memory T

Received 8 July 2024; revised 17 October 2024; accepted 23 October 2024; accepted manuscript published online XXX; corrected proof published online XXX

Cite this article as: JID Innovations 2025;5:100324

© 2024 The Authors. Published by Elsevier Inc. on behalf of the Society for Investigative Dermatology. This is an open access article under the CC BY-NC-ND license (http://creativecommons.org/licenses/by-nc-nd/4.0/).

Table 1. The Demographics of Normal Sun-Protected Truncal Skin Samples

Demographics	Young (n = 20)	Old (n = 30)	*P*-Value
Sex, number of females (percentage females)	20 (100)	30 (100)	N/A
Age, y, median (range)	22.8 (16–28)	61.7 (53–74)	<.001
Number of hair follicle units per millimeter of skin, median (range)	0.13 (0–0.575)	0.128 (0–0.628)	.43
Epidermal thickness, μm, median (range)	40.6 (33.6–59.9)	31.4 (20.3–52.1)	<.001

Abbreviation: N/A, not available.

Specifically, we characterized T cells residing in the epidermis of young and old sun-protected normal skin (Table 1). Most T cells in the epidermis express CD103, a TRM cell marker (Figure 1) (Watanabe et al, 2015). $CD4^+$ and $CD8^+$ T cells were increased in the old compared with those in the young epidermis (Figure 2a–d). LCs were found in direct contact with $CD4^+$ and $CD8^+$ T cells in the epidermis (Figure 2a and b). Interestingly, a higher number of $CD4^+$ and $CD8^+$ T cells contacted LCs in the old compared with those in the young epidermis (Figure 2e and f). The rate of LC–T cell contact was also higher for both $CD4^+$ and $CD8^+$ T cells in the old than in the young epidermis (Figure 2g and h). These results indicate that LCs may interact directly with T cells in the epidermis without migrating to lymph nodes.

LCs contacting T cells express HLA-II^{high}, CD86, and PD-L2

Next, we sought to characterize the LCs that contacted T cells in the old epidermis. HLA-II molecules are expressed on APCs, which present antigens to $CD4^+$ T cells (Couture et al, 2019). As professional APCs, LCs express HLA-II. However, the level of HLA-II expression on APCs varies and is associated with their antigen-presentation capacity (Pishesha et al, 2022). LCs that contacted T cells exhibited higher levels of HLA-II expression than LCs that did not contact T cells (Figure 3a and b). We investigated the expression of costimulatory molecules, CD86 and CD80, on LCs in the old epidermis. A significantly higher percentage of LCs that contacted T cells expressed CD86, whereas CD80 expression was not detectable on LCs regardless of their contact with T cells (Figure 3c–e). Furthermore, we examined immune checkpoint ligand expression on LCs in the old epidermis. Whereas PD-L1 was not detected on epidermal LCs, a significantly higher percentage of LCs that contacted T cells expressed PD-L2 (Figure 4). These findings reveal a combination of ligands expressed by epidermal LCs in contact with T cells, which may imply a biologically meaningful interaction between LCs and T cells in the epidermis.

T cells contacting LCs express CTLA-4, Foxp3, and PD-1

To further elucidate the biological meaning of the contact between LCs and T cells in normal skin, we characterized T cells that contacted LCs in the old epidermis. Given that LCs contacting T cells expressed CD86, we assessed the expression of its receptors, CD28 and CTLA-4, on T cells in the epidermis. CTLA-4 was expressed on $CD4^+$ T cells in the epidermis, whereas CD28 was not detected on T cells in the epidermis (Figure 5a and b). A higher percentage of $CD4^+$ T cells contacting LCs expressed CTLA-4 than $CD4^+$ T cells not contacting LCs (Figure 5c and d). CTLA-4 is mostly expressed by $CD4^+$ regulatory T cells (Tregs) (Friedline et al, 2009). Consistently, we found that a higher percentage of $CD4^+$ T cells contacting LCs expressed the Treg-associated transcription factor, Foxp3 (Figure 5e and f). More specifically, we found that LCs contacted CTLA-4^+Foxp3^+ Tregs in the epidermis, and most CTLA4^+CD4^+ T cells in the epidermis were Foxp3^+ Tregs (Figure 6a–d). Interestingly, Tregs in the epidermis express the tissue-resident marker, CD103 (Figure 6e). With regard to PD-L2 expression on LCs contacting T cells, we found that $CD4^+$ and $CD8^+$ T cells in the epidermis broadly express PD-1 regardless of their contact with LCs (Figure 7). These results imply that the interaction between LCs and T cells in the epidermis has a regulatory nature, blocking TRM cell activation through the engagement of CD86/CTLA-4 and PD-L2/PD-1 checkpoints.

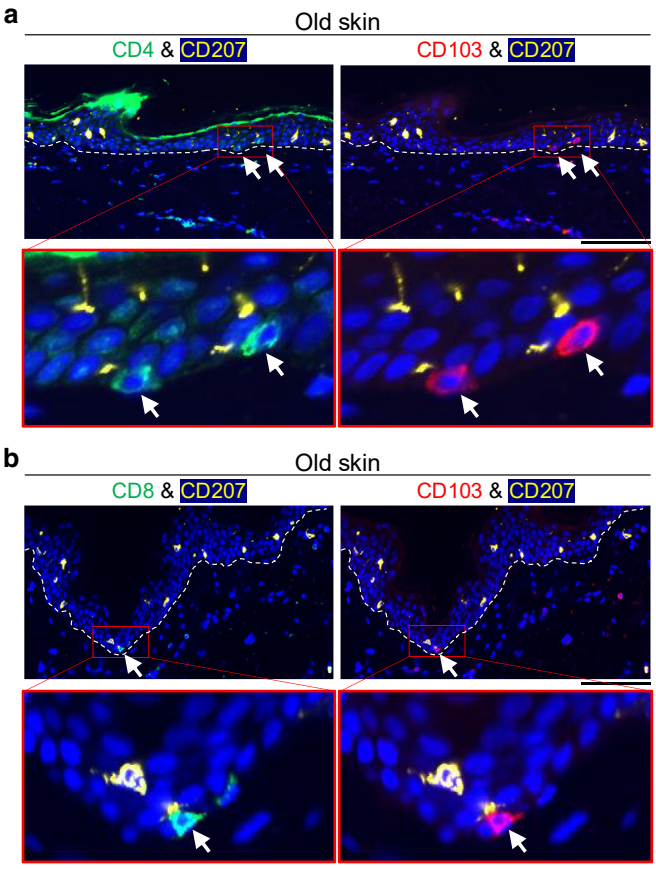

Figure 1. T cells in the epidermis express tissue-resident memory marker. (**a, b**) Representative images of (**a**) CD4/CD103/CD207- and (**b**) CD8/CD103/CD207-stained young and old human skin. White arrows indicate $CD103^+$ T cells in the epidermis. White dashed lines indicate the basement membrane. Bars = 100 μm.

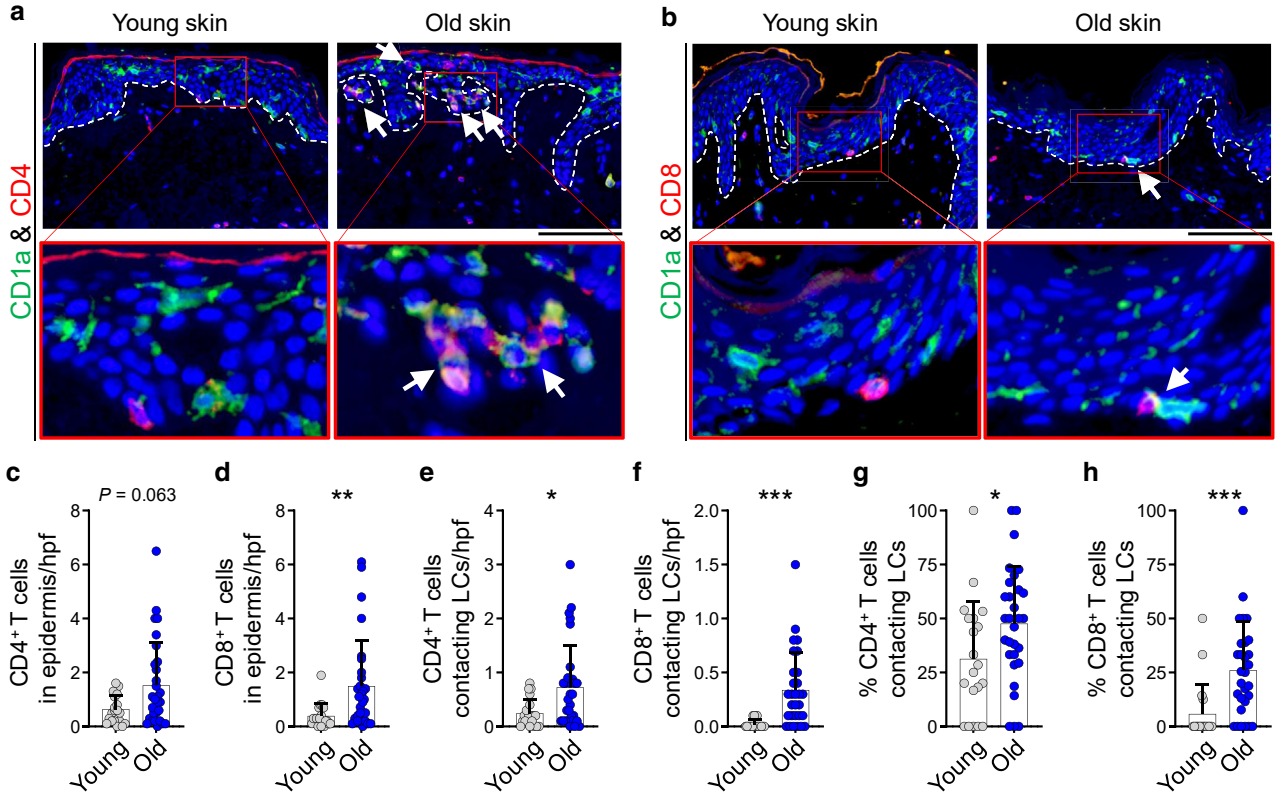

Figure 2. LC–T cell contact in the epidermis is increased with aging. (**a, b**) Representative images of CD1a/CD4- and CD1a/CD8-stained young and old sun-protected human skin. Note that $CD4^+$ and $CD8^+$ cells are $CD3^+$ T cells. White arrows point to LC–T cell contact. White dashed lines indicate the basement membrane. (**c, d**) Quantification of (**c**) $CD4^+$ T cells and (**d**) $CD8^+$ T cells in the epidermis per hpf images of young and old human skin. (**e, f**) Quantification of (**e**) $CD4^+$ T and (**f**) $CD8^+$ T cells contacting LCs in the epidermis per hpf images of young and old human skin. (**g, h**) Percentage (**g**) $CD4^+$ T and (**h**) $CD8^+$ T cells contacting LC per total $CD4^+$ T and $CD8^+$ T cells in the epidermis in young versus old human skin. Bar graphs show mean + SD, n = 20 young skin and n = 30 old skin samples, Mann–Whitney *U* test. Bars = 100 μm. $^*P < .05$, $^{**}P < .01$, and $^{***}P < .001$. hpf, high power field; LC, Langerhans cell.

Inflammatory insults decrease HLA-II and CD86 on epidermal LCs

To examine whether HLA-II and CD86 expression on epidermal LCs associated with a tolerogenic state, we developed an ex vivo platform to expose skin to inflammatory insults and observe their impact on LC phenotype in the epidermis (Figure 8a). Normal skin samples exposure to an inflammatory dose 345 mJ/cm^2 of UVB radiation for 24 hours resulted in LC migration to the basal layer (Figure 8b and c) (Kölgen et al, 2002). Interestingly, the percentage of HLA-II^{low} and $CD86^-$ LCs in the basal layer significantly increased after UVB irradiation (Figure 8b, d, and e). To test another inflammatory insult, skin samples were treated with 2,4-dinitrofluorobenzene (DNFB), a topical hapten known to induce contact hypersensitivity (Moorhead, 1978). Similar to UVB, DNFB treatment triggered LC migration to the epidermal basal layer (Figure 8f and g). Furthermore, the percentage of HLA-II^{low} and $CD86^-$ LCs in the basal layer significantly increased after DNFB application (Figure 8f, h, and i). Our findings indicate that inflammatory insults disrupt the tolerogenic balance in the epidermis by downregulating CD86 and HLA-II expression in LCs.

ICB therapy blocks LC–T-cell interaction in the epidermis

ICB therapy can induce cutaneous immune-related adverse events (cirAEs) in patients with cancer (Nadelmann et al, 2022). Our research suggested that LC–T-cell interaction in the epidermis contributed to immunological tolerance under normal conditions through the CD86/CTLA-4 and PD-L2/PD-1 pathways. Therefore, we hypothesized that the ICB might result in cirAE, at least in part, by disrupting the LC–T-cell regulatory axis in the epidermis. To investigate this possibility, we assessed LC–T-cell contact in the normal truncal skin of patients with cancer on PD-1 blockade therapy who developed cirAEs. The median duration of ICB therapy was 173 days, with a range of 19–2133 days. LC–T-cell contact rate was markedly reduced in anti–PD-1 antibody-treated normal skin compared with that in the normal truncal skin from age- and sex-matched healthy donors (Figure 9 and Table 2). This observation supports the tolerogenic function of LC–T-cell interaction in the epidermis, the loss of which may contribute to cirAE development in patients with cancer receiving ICB therapy.

DISCUSSION

Our findings reveal a direct interaction between LCs and TRM cells in the epidermis that may contribute to skin homeostasis. We demonstrate that LCs engage with TRM cells more frequently in the epidermis of old individuals. LCs that contact T cells in the epidermis are marked by high expression of HLA-II, CD86, and PD-L2. In turn, T cells that contact LCs express CTLA-4, Foxp3, and PD-1. This ligand/receptor expression pattern suggests that the LC–T-cell interaction in

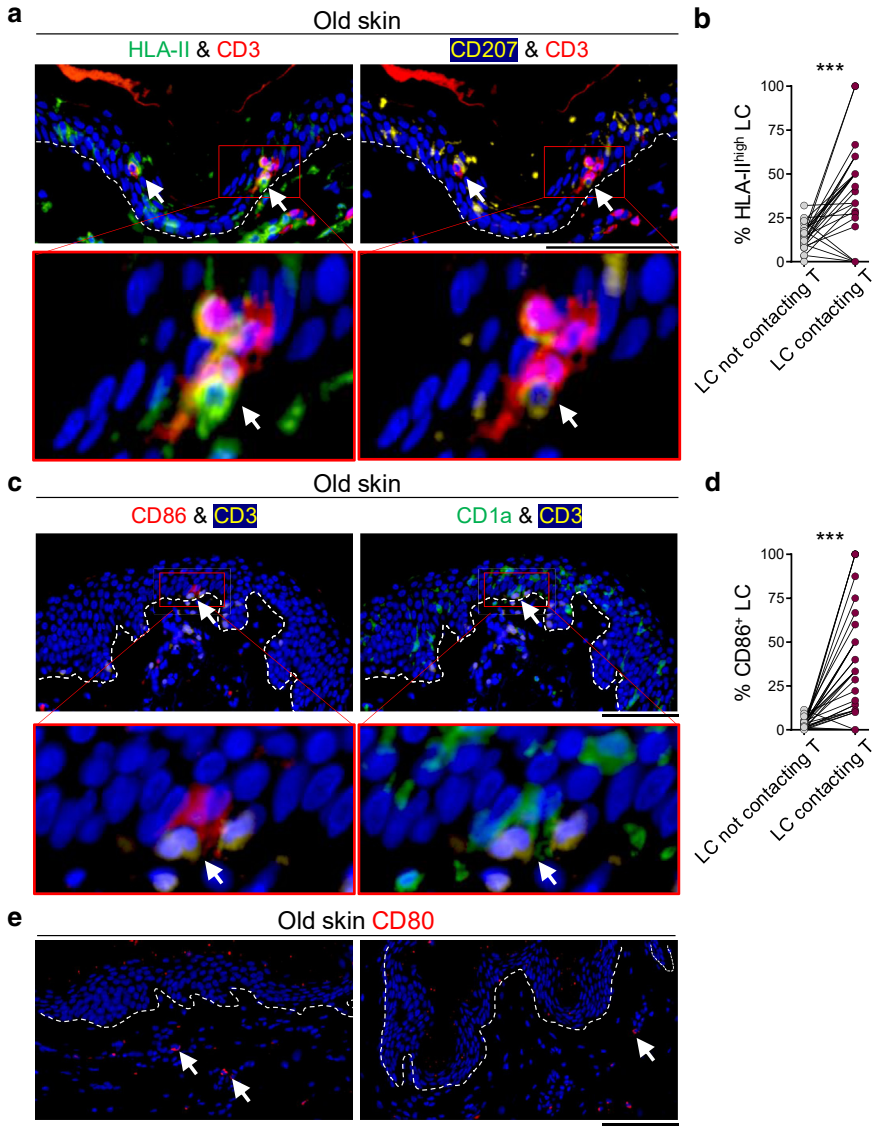

Figure 3. LCs contacting T cells express HLA-II^{high} and CD86. (**a**) Representative images of HLA-II/CD207/CD3−stained old human skin. (**b**) Percentage HLA-II^{high} LCs of LCs that are contacting versus not contacting T cells in the epidermis. (**c**) Representative images of CD86/CD1a/CD3-stained old human skin. (**d**) Percentage CD86^{+} LCs of LCs that are contacting versus not contacting T cells in the epidermis. (**e**) Representative images of CD80-stained old human skin. White arrows indicate CD80^{+} cells in the dermis. White dashed lines indicate the basement membrane. n = 30 old skin samples, paired *t*-test. Bars = 100 μm. ***$P < .001$. LC, Langerhans cell.

the normal epidermis is tolerogenic. Furthermore, we demonstrate that established immune stimulants disrupt the LC−T cell tolerogenic axis by downregulating HLA-II and CD86 on LCs. Likewise, PD-1 blockade blocks LC−T cell contact in the normal epidermis of patients with cancer with cirAEs. Our discovery sheds light on a previously unrecognized role of LCs in maintaining immune tolerance through direct interactions with Tregs and TRM cells residing in the epidermis.

Human skin contains a substantial population of TRM cells, a significant portion of which are targeted at normal skin microbial flora (Clark, 2010, 2006). The interaction between LCs and TRM cells in the epidermis contributes to regulating TRM cell activation and maintaining tolerance to our commensal microbiome. Our findings also indicate that epidermis-resident Tregs interact with LCs to maintain skin homeostasis. Although the functions of skin-resident Tregs are not fully understood, previous studies have examined the immunoregulatory role of skin-resident Tregs (Rosenblum et al, 2011; Seneschal et al, 2012). LCs induce activation and proliferation of skin-resident Tregs in the absence of a foreign pathogen in vitro (Seneschal et al, 2012). Thymus-derived Tregs become activated upon expression of self-antigen and are maintained and primed to attenuate subsequent autoimmune reactions in the epidermis (Rosenblum et al, 2011). The precise regulation of TRM cells remains incompletely understood. One plausible mechanism involves antigen dosage: when commensal antigens surpass a certain threshold, they trigger TRM cell activation, whereas at doses below the threshold, Treg activation is induced (Seneschal et al, 2012). LCs are the APCs of the epidermis that can govern this process, and their direct contact with TRM cells and Tregs supports this role. Interestingly, recent single-cell transcriptome analysis has revealed that LCs exist in 2 steady states in the epidermis, one of which is immunomodulatory and induces Tregs (Liu et al, 2021). Downregulation of HLA-II and CD86 on LCs by UVB and DNFB supports the disruption in the tolerogenic axis between LCs and T cells (Kölgen et al, 2002; Nakagawa et al, 1999; Rambukkana et al, 1996; Rattis et al, 1998).

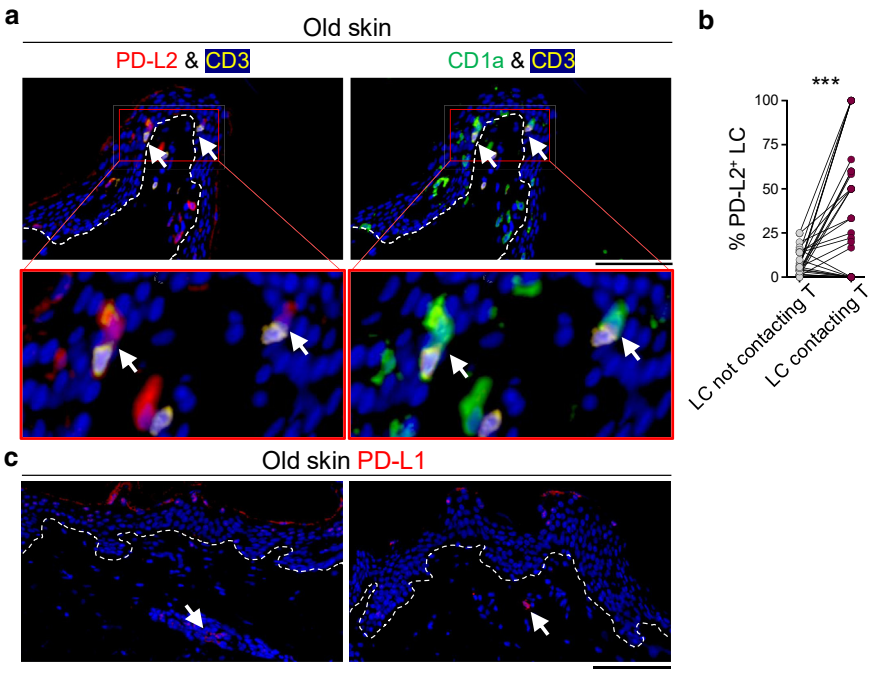

Figure 4. LCs contacting T cells express PD-L2. (**a**) Representative images of PD-L2/CD1a/CD3−stained old human skin. (**b**) Percentage PD-L2$^+$ LCs of LCs that are contacting versus not contacting T cells in the epidermis. White arrows point to LC−T-cell contact. (**c**) Representative images of PD-L1−stained old human skin. White dashed lines indicate the basement membrane. n = 30 old skin samples, paired *t*-test. Bars = 100 μm. ***$P < .001$. LC, Langerhans cell.

TRM cells possess proinflammatory and regulatory properties (Kumar et al, 2017). When TRM cells encounter exogenous antigens expressed by pathogens, they become activated to eliminate the threat (Kamenjarin et al, 2023). It stands to reason that TRM cells would be poised for deactivation when encountering physiological levels of exogenous antigens expressed by normal flora of the skin. In old skin, there are significantly more LC−T cell interactions than in young skin. Given that old skin has experienced greater exposure to environmental stimuli, more LC−T cell interactions may play a crucial role in its maintenance. Our finding that PD-1$^+$ TRM cells reside in contact with PD-L2$^+$ LCs in the healthy human epidermis supports this concept. PD-1 plays a critical role in CD8$^+$ TRM cell peripheral tolerance (Gamradt et al, 2019). Considering the normal, noninflamed nature of the skin samples studied, the interaction between PD-L2$^+$ LCs and PD-1$^+$ conventional T cells also points to maintaining CD4$^+$ T cell tolerance in the epidermis. Furthermore, the PD-1/PD-L2 axis plays an important role in maintaining Treg stability and immunosuppressive functions in the context of peripheral tolerance (Hurrell et al, 2022). Although we cannot rule out the possibility that cancer may reduce LC−T cell contact in the epidermis, our research indicates that PD-1 blockade results in diminished LC−T cell contact within normal skin. This observation suggests that the normal skin in patients who experience cirAEs may be predisposed to an overactive TRM cell response, attributable to the disruption of the regulatory LC−T cell axis caused by PD-1 blockade. Our findings are supported by the critical function of PD-1 in the skin to maintain CD8$^+$ T cell tolerance toward cutaneous antigens (Damo et al, 2023).

In conclusion, our findings provide a unique perspective on the role of LC in maintaining skin tolerance within the epidermis. Our findings indicate that LCs, which are the professional APCs in the epidermis, may possess the capability to maintain tolerance without the necessity of migration to lymph nodes. This study illuminates the fundamental role of tissue-specific APCs in the preservation of peripheral tolerance.

MATERIALS AND METHODS

Human skin tissue study

The study of deidentified normal adult human skin samples was reviewed and approved by the Institutional Review Board. Patient consent for experiments was not required because the United States laws consider human tissue left over from surgery as discarded material. After surgery, the discarded skin samples were stored in sterile RPMI 1640 medium (Thermo Fisher Scientific, Waltham, MA, 21-870-092) at 4 °C and processed within 6 hours. Normal breast skin samples from female donors were used to characterize LC−T-cell interactions (Table 1). Normal breast and abdominal skin samples from female donors were used for ex vivo studies. Studies on cirAE-associated skin samples were reviewed and approved by the Institutional Review Board (Table 2). Patient's written, informed consent was obtained according to Institutional Review Board protocol. Deidentified normal abdominal skin samples from male and female donors were used as age- and sex-matched healthy donor samples for cirAE-related studies (Table 2). One investigator was responsible for counting the cells in the human skin tissue studies.

Histology

Tissue samples were fixed with 4% paraformaldehyde and embedded in paraffin. A total of 5-μm sections were cut and deparaffinized. After being permeabilized with 0.2% Triton-X (Thermo Fisher Scientific, BP151) in PBS for 5 minutes, antigen retrieval was performed using a pressure cooker in citrate-based antigen unmasking solution (Vector Laboratories, Burlingame, CA, H-3300-250) or tris-based antigen unmasking solution (Vector Laboratories, H-3301-250) for 20 minutes. Slides were rinsed once in deionized water and in PBS with 0.1% Tween 20 (Sigma-Aldrich, St.

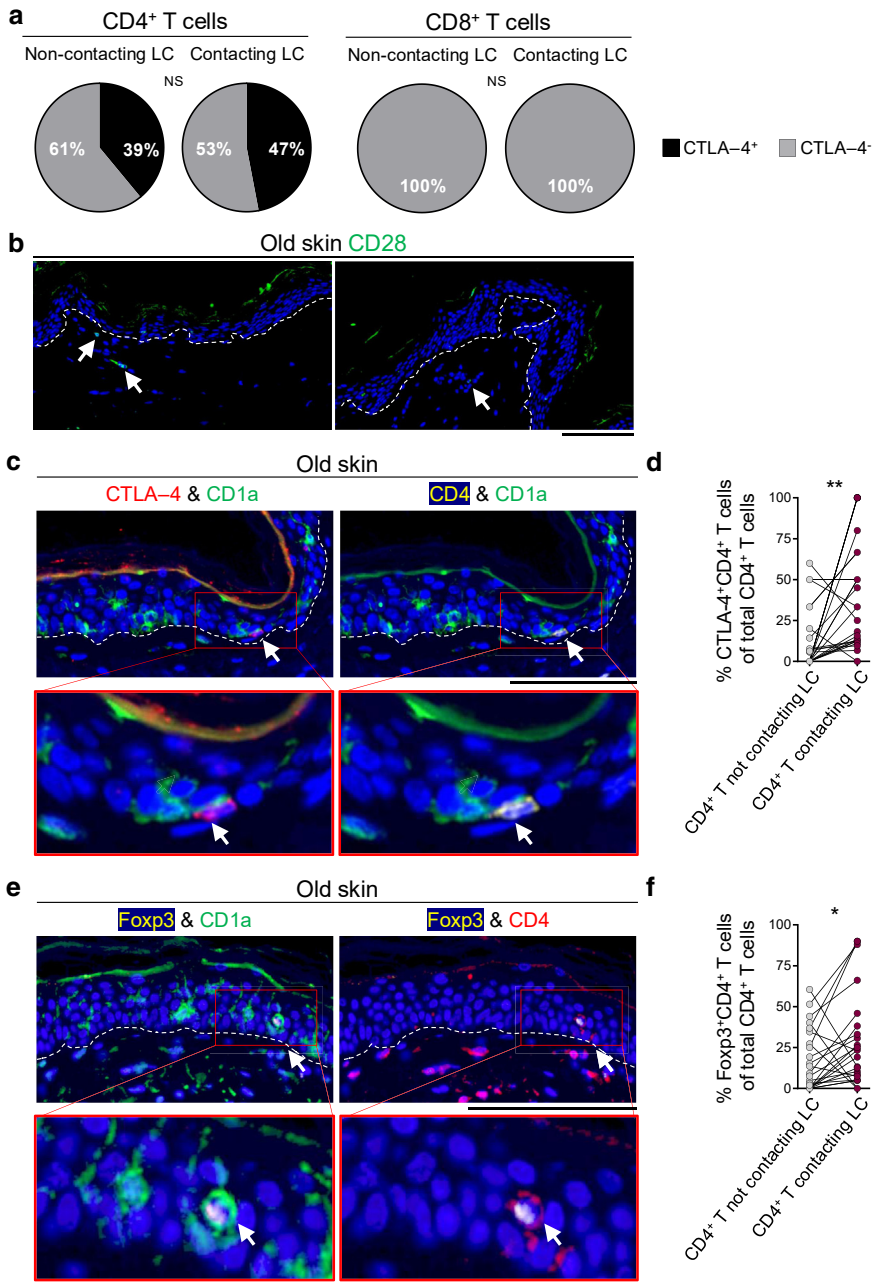

Figure 5. T cells contacting LCs express CTLA-4 and Foxp3. (**a**) Percentage CTLA-4$^+$ cells of CD4$^+$ and CD8$^+$ T cells that are contacting versus not contacting LCs in the epidermis of old human skin. n = 30 old skin samples (for CD4$^+$ T cells), and n = 3 old skin samples (for CD8$^+$ T cells). (**b**) Representative images of CD28-stained old human skin. White arrows indicate CD28$^+$ cells in the dermis. (**c**) Representative images of CTLA-4/CD4/CD1a–stained old human skin. (**d**) Percentage CTLA-4$^+$CD4$^+$ T cells of CD4$^+$ T cells that are contacting versus not contacting LCs in the epidermis. (**e**) Representative images of Foxp3/CD1a/CD4-stained old human skin. (**f**) Percentage Foxp3$^+$CD4$^+$ T cells of CD4$^+$ T cells that are contacting versus not contacting LCs in the epidermis. Note that CD4$^+$ cells are CD3$^+$ T cells. n = 30 old skin samples, chi-square test (for **a**) and paired *t*-test (for **d** and **f**). Bars = 100 μm. *P < 005 and **P < .01. LC, Langerhans cell; NS, not significant.

Louis, MO, P1379). Slides were blocked with 5% normal goat serum (Sigma-Aldrich, G9023) in PBS and incubated in a humidified chamber at room temperature for 1 hour. Slides were incubated overnight at 4 °C with primary antibodies diluted in the blocking buffer (Table 3). When stained with 2 primary antibodies from the same host species, signal amplification and heat-induced stripping for antibodies were done following the standard protocol using Opal 4-Color IHC Kit (PerkinElmer, Waltham, MA, NEL820001KT). After primary antibody application, slides were rinsed once and washed 3 times for 2 minutes each in PBS with 0.1% Tween 20. Slides were incubated in secondary antibodies (Table 3) and DAPI (Thermo Fisher Scientific, D3571, 1:4000) diluted in the blocking buffer for 20 minutes at room temperature. Slides were washed in PBS with 0.1% Tween 20 and mounted with Fluoroshield (Sigma-Aldrich, F6182). The stained tissues were imaged with a ZEISS Axio Scan.Z1 Slide Scanner (Zeiss, Oberkochen, Germany). For H&E staining, slides were stained according to standard procedures and mounted with Cytoseal XYL (Thermo Fisher Scientific, 8312-4).

Image analysis

Cell counts were done across up to 10 randomly selected high-power field images across 15-mm skin length on average for normal skin tissue. Cell–cell distance was measured by Halo 3.0 software (Indica Labs, Albuquerque, NM). When cell-to-cell distance was <12 μm, cells were determined to be contacting each other. The cut offs for HLA-II^{high} were determined to be 75% of the average HLA-II signal of the dermal HLA-II$^+$ cells by Halo 3.0 software (Indica Labs).

Ex vivo experiments

A total of 8-mm punch biopsies from normal adult truncal skin were used for ex vivo studies. For UVB radiation, we exposed the skin samples to low-intensity UVB radiation continuously for 24

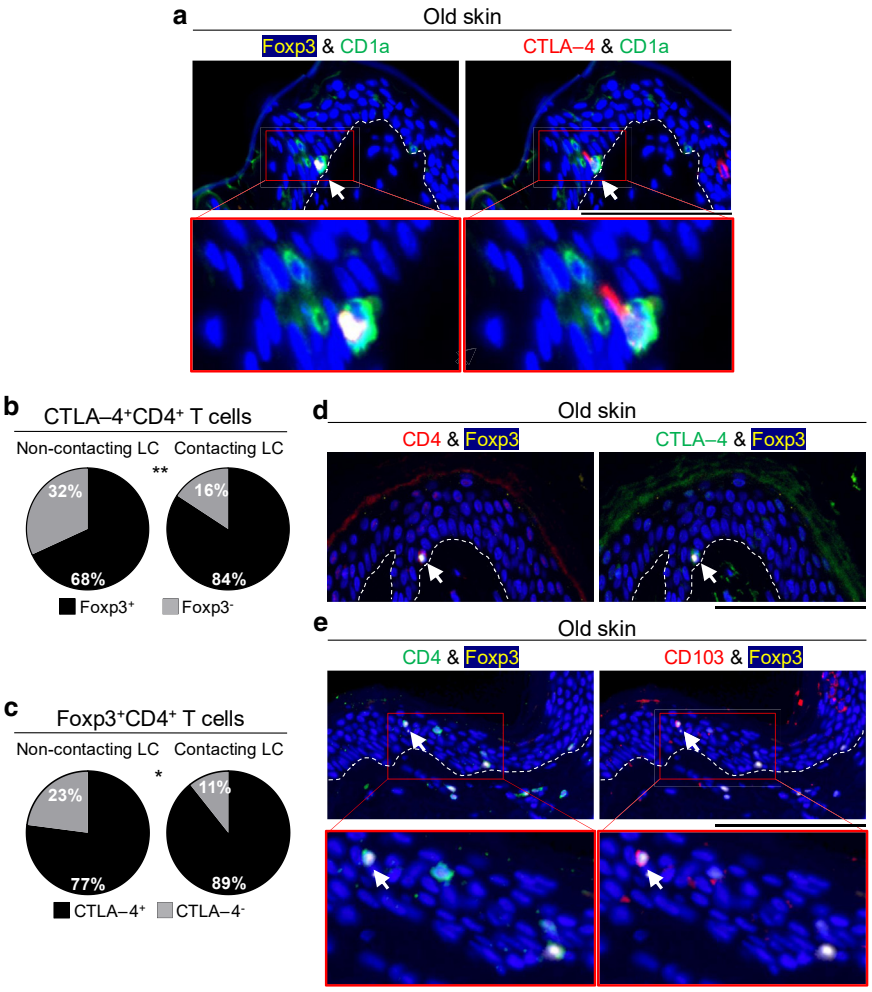

Figure 6. CTLA-4$^+$Foxp3$^+$ Tregs contact LCs. (**a**) Representative images of Foxp3/CTLA-4/CD1a–stained old human skin. White arrows point to CTLA-4$^+$Foxp3$^+$ cell–LC contact. Note that CTLA-4$^+$Foxp3$^+$ cell is CD4$^+$ Treg. (**b**) Percentage of Foxp3$^+$ cells of CTLA-4$^+$CD4$^+$ T cells that are contacting versus not contacting LCs in the epidermis. n = 30 old skin samples. (**c**) Percentage of CTLA-4$^+$ cells of Foxp3$^+$CD4$^+$ T cells that are contacting versus not contacting LCs in the epidermis. n = 30 old skin samples. (**d**) Representative images of CD4/CTLA-4/Foxp3–stained old human skin. White arrows point to CTLA-4$^+$Foxp3$^+$CD4$^+$ Treg. (**e**) Representative images of CD4/CD103/Foxp3-stained old human skin. White arrows point to CD103$^+$Foxp3$^+$CD4$^+$ Treg. White dashed lines indicate the basement membrane. Chi-square test was used. Bars = 100 μm. *$P < .05$ and **$P < .01$. LC, Langerhans cell; Treg, regulatory T cell.

hours during culture, receiving a total dose of 345 mJ/cm^2 UVB or sham radiation. For DNFB application, skin biopsies received 20 μl of 0.2% DNFB or vehicle control (combination of acetone and olive oil at 4:1 volume ratio) on the surface of the epidermis prior to being transferred to the air–liquid interface of the culture medium. Biopsied samples were incubated at the air–liquid interface in RPMI 1640 medium (Thermo Fisher Scientific) with 10% fetal bovine serum, 1% penicillin/streptomycin, and 1%

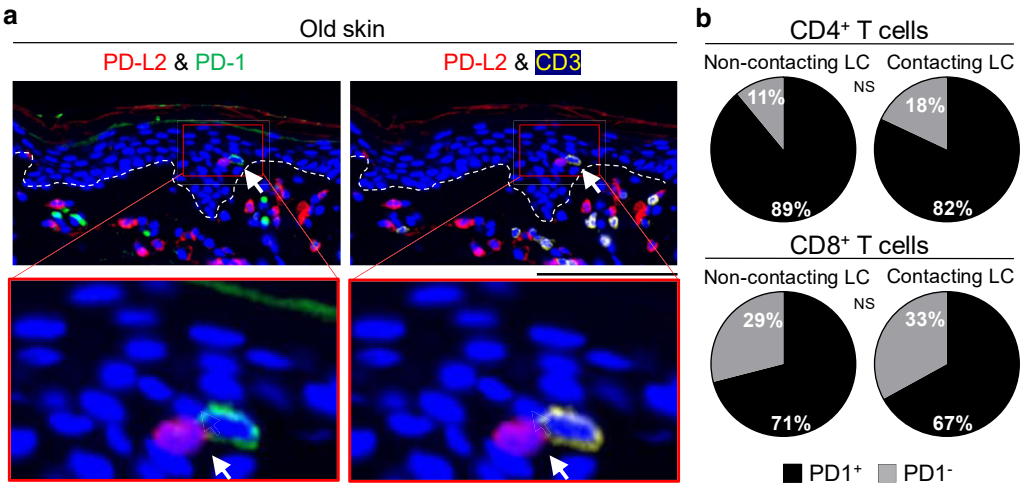

Figure 7. Epidermal T cells express PD-1. (**a**) Representative images of PD-L2/PD-1/CD3–stained old human skin. White arrows indicate LC–T cell contact. White dashed lines indicate the basement membrane. (**b**) Percentage of PD-1$^+$ CD4$^+$ and CD8$^+$ T cells that are contacting versus not contacting LCs in the epidermis. n = 30 old skin samples, chi-square test. Bar = 100 μm. LC, Langerhans cell; NS, not significant.

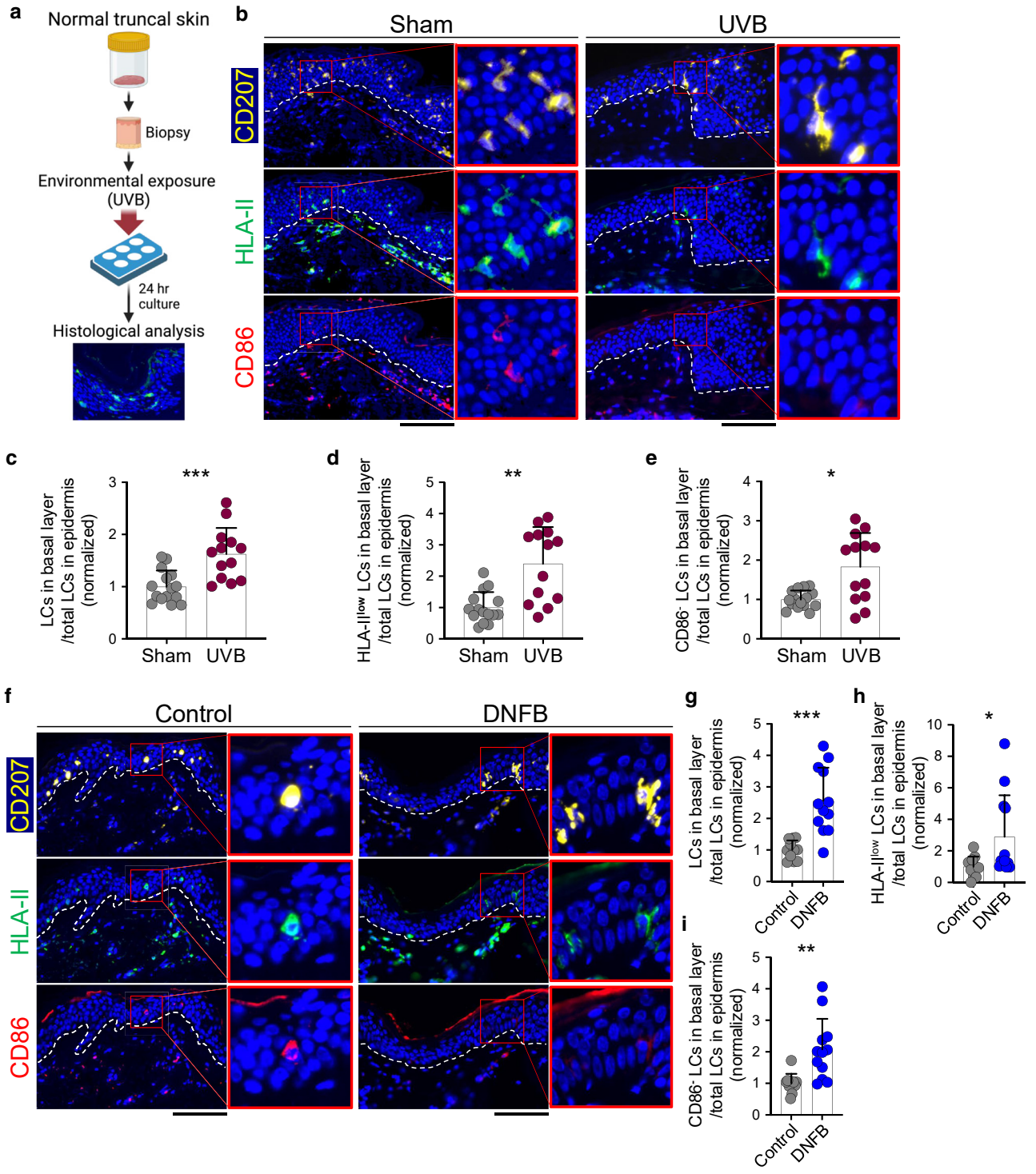

Figure 8. UVB and DNFB disrupt the interaction between LCs and T cells in the epidermis. (**a**) Schematic diagram of the experimental procedure for ex vivo skin studies. (**b**) Representative images of CD207/HLA-II/CD86–stained skin treated ex vivo with 345 mJ/cm^2 UVB or sham radiation over 24 hours. (**c**–**e**) Quantification of (**c**) LCs in basal layer per total LCs, (**d**) HLA-II^{low} LCs in basal layer per total LCs, and (**e**) CD86$^-$ LCs in basal layer per total LCs normalized across skin samples. n = 14 skin samples from 4 donors in UVB, and n = 16 skin samples from 4 donors in sham group. (**f**) Representative images of CD207/HLA-II/CD86–stained skin after DNFB versus carrier control treatment ex vivo. (**g**–**i**) Quantification of (**g**) LCs in basal layer per total LCs, (**h**) HLA-II^{low} LCs in basal layer per total LCs, and (**i**) CD86$^-$ LCs in basal layer per total LCs normalized across skin samples. n = 12 skin samples from 4 donors in DNFB, and n = 11 skin samples from 4 donors in the control group. White dashed lines indicate the basement membrane. Bar graphs show mean + SD, Mann–Whitney *U* test. Bars = 100 μm. *$P < .05$, **$P < .01$, and ***$P < .001$. DNFB, 2,4-dinitrofluorobenzene; LC, Langerhans cell.

glutamine at 37 °C under an atmosphere of 5% carbon dioxide in the air. Twenty-four hours after incubation, we collected the samples and analyzed them by immunofluorescence staining. We identified the LC as being on the basal layer when its nucleus was positioned at the same level as other keratinocytes in the basal layer, which was just above the basement membrane. We

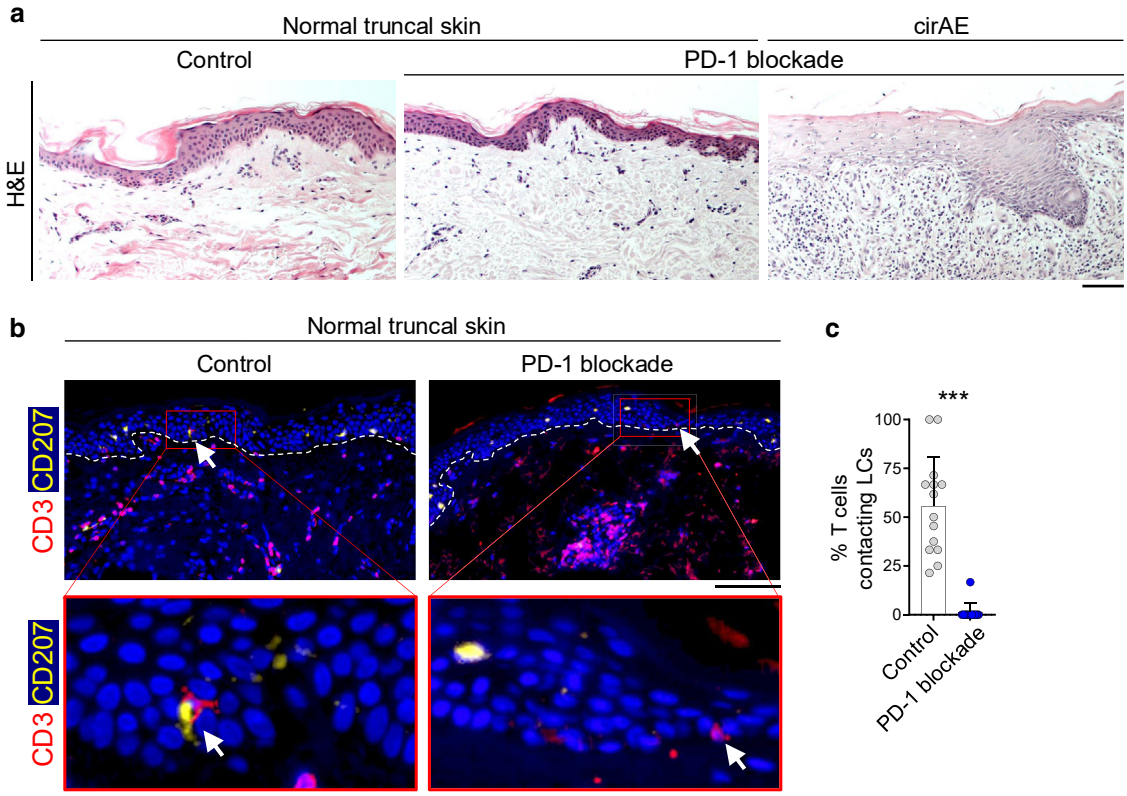

Figure 9. ICB disrupts the interaction between LCs and T cells in the epidermis. (**a**) Representative images of H&E-stained normal truncal skin from a healthy donor, normal truncal skin from a patient with cancer receiving PD-1 blockade, and cirAE biopsy from the same patient. (**b**) Representative images of CD3/CD207-stained normal truncal skin from patients with cancer who received PD-1 blockade and developed cirAEs compared with those of normal truncal skin from age- and sex-matched healthy donors (controls). (**c**) Percentage of $CD3^+$ T cells contacting LC per total $CD3^+$ T cells in the epidermis of normal truncal skin from patients with cancer who received PD-1 blockade versus controls. n = 12 in PD-1 blockade group, and n = 14 in control group. White dashed lines indicate the basement membrane. Bar graphs show mean + SD, Mann–Whitney *U* test. Bars = 100 μm. ***$P < .001$. cirAE, cutaneous immune-related adverse event; ICB, immune checkpoint blockade; LC, Langerhans cell.

Table 2. The Demographics of the Patients Treated with PD-1 Blockade and the Controls

Demographics	Control (n = 14)	Patients with Cancer Treated with PD-1 Blockade (n = 12)
Sex, number of females (percentage of females)	12 (85.7)	10 (83.3)
Age, y, median (range)	58.8 (49–73)	60.2 (31–86)
Type of cancer, n (%)		
Malignant melanoma	—	5 (41.7)
Nonsmall cell lung cancer	—	2 (16.7)
Squamous cell carcinoma	—	2 (16.7)
Breast cancer	—	1 (8.3)
Pituitary macroadenoma	—	1 (8.3)
Hepatocellular carcinoma	—	1 (8.3)
Type of immune checkpoint blockade, n (%)		
Pembrolizumab	—	7 (58.3)
Nivolumab + ipilimumab	—	3 (25.0)
Nivolumab	—	1 (8.3)
Cemiplimab	—	1 (8.3)

Table 3. Key Resources List

Reagent or Resources	Source	Identifier	Dilution
Histology antibodies			
Human primary antibodies			
CD3	Abcam	Cat# ab11089; RRID: AB_2889189	500
CD3	Cell Signaling Technology	Cat# 85061; RRID: AB_2721019	200
CD4	Thermo Fisher Scientific	Cat# MA1-39582; RRID: AB_10986805	200
CD8	Cell Signaling Technology	Cat# 70306; RRID: AB_2799781	500
CD1a	Dako	Cat# M3571; RRID: AB_2073290	500
CD28	Abcam	Cat# ab113358; RRID: AB_10861658	500
CD80	Sigma-Aldrich	Cat# HPA050092; RRID: AB_2681012	100
CD86	Cell Signaling Technology	Cat# 91882; RRID: AB_2797422	500
CTLA-4	Abcam	Cat# ab237712; RRID: AB_2905652	200
CD103	Abcam	Cat# ab129202; RRID: AB_11142856	500
CD207	Novus Biologicals	Cat# DDX0362P; RRID: AB_2892751	500
PD-1	Cell Signaling Technology	Cat# 86163; RRID: AB_2728833	100
PD-L1	Cell Signaling Technology	Cat# 13684; RRID: AB_2687655	100
PD-L2	Cell Signaling Technology	Cat# 82723; RRID: AB_2799999	100
HLA-DP, DQ, DR (HLA-II)	Dako	Cat# M0775; RRID: AB_2313661	1000
Foxp3	eBioscience	Cat# 14-4776; RRID: AB_2865086	500
Secondary antibodies			
Goat anti Mouse IgG (H+L), Multi-Species SP ads-AF488	SouthernBiotech	Cat# 1038-30; RRID: AB_2794366	200
Goat anti Rabbit IgG (H+L) Antibody, Alexa Fluor 568	Abcam	Cat# ab175471; RRID: AB_2576207	200
Goat anti Rat IgG (H+L) Highly Cross-Adsorbed Secondary Antibody, Alexa Fluor Plus 647	Thermo Fisher Scientific	Cat# A48265; RRID: AB_2895299	200
Goat anti Rabbit IgG (H+L) Highly Cross-Adsorbed Secondary Antibody, Alexa Fluor 488	Thermo Fisher Scientific	Cat# A11034; RRID: AB_2576217	200
Histology reagents			
Paraformaldehyde	Sigma-Aldrich	Cat# P6148	—
Triton-X	Thermo Fisher Scientific	Cat# BP151	—
Citrate-Based Antigen Unmasking Solution	Vector Laboratories	Cat# H-3300-250	—
Tris-Based Antigen Unmasking Solution	Vector Laboratories	Cat# H-3301-250	—
Tween 20	Sigma-Aldrich	Cat# P1379	—
Normal goat serum	Sigma-Aldrich	Cat# G9023	—
BSA	Thermo Fisher Scientific	Cat# BP1600	—
DAPI	Thermo Fisher Scientific	Cat# D3571	—
Fluoroshield histology mounting medium	Sigma-Aldrich	F6182-20ML	—
Cytoseal XYL	Thermo Fisher Scientific	Cat# 8312-4	—
Opal 4-Color IHC Kit	PerkinElmer	Cat# NEL820001KT	—
Hematoxylin	Sigma-Aldrich	Cat# GHS132-1L	—
Eosin	Leica Biosystems	Cat# 380619	—
Ex vivo study reagents			

(*continued*)

Table 3. Continued

Reagent or Resources	Source	Identifier	Dilution
RPMI 1640	Thermo Fisher Scientific	Cat# 21-870-092	—
2,4-dinitrofluorobenzene	Sigma-Aldrich	Cat# 556971	—
Software and algorithms			
Zen Blue 3	Zeiss	https://www.zeiss.com/microscopy/en/products/software/zeiss-zen.html	—
NDP.View2	Hamamatsu Photonics	https://www.hamamatsu.com/jp/en/product/life-science-and-medical-systems/digital-slide-scanner/U12388-01.html	—
Prism 10.3.1	GraphPad	https://www.graphpad.com/scientific-%20software/prism/	—
Biorender	BioRender	https://biorender.com/	—
Halo AI	Indica Labs	https://indicalab.com/halo-ai/	—
Equipment			
Zeiss Axio Observer Z1	Zeiss	N/A	—
Zeiss Axio Scan.Z1	Zeiss	N/A	—
UVP XX-Series Bench Lamp 115V	Thermo Fisher Scientific	UVP95004208	—
Hand-Held Light Meter	International Light Technologies	ILT2400	—

Abbreviations: Cat#, catalog number; N/A, not available; RRID, Research Resource Identifier.

normalized the data within each set of samples obtained from a single donor, ensuring that the average of the control samples from each donor equaled 1. After we normalized the data in 1 donor, we combined normalized data across the donors in the study to generate the graphs. One investigator was responsible for counting in the human skin tissue study.

Quantification and statistical analysis

All bar graphs and dot plots show mean + SD. A 2-tailed Mann–Whitney *U* test was used for comparisons between groups. A 2-tailed paired *t*-test was used for within-group comparisons. The chi-square test was used to compare categorical data represented in pie charts. GraphPad Prism 10 (GraphPad Software, Boston, MA) was used for statistical analysis. $P < .05$ was considered statistically significant.

ETHICS STATEMENT

The study of deidentified normal adult truncal skin samples from female donors was reviewed and approved by the Institutional Review Board at Massachusetts General Hospital. Patient consent for the analyses using the deidentified samples was not required because the United States laws consider human tissue left over from surgery as discarded material. Studies on cutaneous immune-related adverse event–associated skin samples were reviewed and approved by the Massachusetts General Hospital Institutional Review Board. Patient's written, informed consent was obtained according to Institutional Review Board protocol.

DATA AVAILABILITY STATEMENT

The data supporting this study's findings are available from the corresponding author upon reasonable request.

ORCIDs

Tomonori Oka: http://orcid.org/0000-0001-7362-3207
Tatsuya Hasegawa: http://orcid.org/0000-0001-7310-786X
Truelian Lee: http://orcid.org/0000-0002-5364-7022
Valeria S. Oliver-Garcia: http://orcid.org/0000-0002-9435-6731
Mahsa Mortaja: http://orcid.org/0000-0002-8503-9806
Marjan Azin: http://orcid.org/0000-0001-6950-4854
Satoshi Horiba: http://orcid.org/0000-0002-7047-0097
Sabrina S. Smith: http://orcid.org/0000-0002-4234-1458
Sara Khattab: http://orcid.org/0000-0002-4724-258X
Kathryn E. Trerice: http://orcid.org/0000-0003-1119-6734
Steven T. Chen: http://orcid.org/0000-0001-8844-3284
Yevgeniy R. Semenov: http://orcid.org/0000-0002-7387-3094
Shadmehr Demehri: http://orcid.org/0000-0002-7913-2641

CONFLICT OF INTEREST

The authors state no conflict of interest.

ACKNOWLEDGMENTS

SD holds a Career Award for Medical Scientists award from the Burroughs Wellcome Fund. TH and SH were supported by Shiseido. The authors gratefully acknowledge support from Shiseido. The graphical abstract and schematic diagrams were created with biorender.com. Tissue samples were provided by the Cooperative Human Tissue Network, which is funded by the National Cancer Institute. Other investigators may have received specimens from the same subjects.

AUTHOR CONTRIBUTIONS

Conceptualization: TO, TH, SD; Data Curation: TO, TH, TL, VSO-G, MM, MA, SH, SSS, KET; Formal Analysis: TO, TH, TL, VSO-G, MM, MA, SH, SSS, KET, SD; Funding Acquisition: SD; Investigation: TO, TH, TL, VSO-G, MM, MA, SH, SSS, SK, KET, STC, YRS, SD; Methodology: TO, TH, SD; Project Administration: TO, SD; Resources: TO, STC, YRS, SD; Supervision: TO, STC, YRS, SD; Validation: TO, TL, SH, SD; Visualization: TO, SD; Writing - Original Draft Preparation: TO; Writing - Review and Editing: TL, VSO-G, SH, SSS, SD

DECLARATION OF GENERATIVE ARTIFICIAL INTELLIGENCE (AI) OR LARGE LANGUAGE MODELS (LLMS)

The authors did not use AI/LLM in any part of the research process and/or manuscript preparation.

REFERENCES

Clark RA. Skin-resident T cells: the ups and downs of on site immunity. J Invest Dermatol 2010;130:362–70.

Clark RA, Chong B, Mirchandani N, Brinster NK, Yamanaka K, Dowgiert RK, et al. The vast majority of CLA+ T cells are resident in normal skin. J Immunol 2006;176:4431–9.

Couture A, Garnier A, Docagne F, Boyer O, Vivien D, Le-Mauff B, et al. HLA-class II artificial antigen presenting cells in $CD4^+$ T cell-based immunotherapy. Front Immunol 2019;10:1081.

Damo M, Hornick NI, Venkat A, William I, Clulo K, Venkatesan S, et al. PD-1 maintains CD8 T cell tolerance towards cutaneous neoantigens. Nature 2023;619:151–9.

Friedline RH, Brown DS, Nguyen H, Kornfeld H, Lee J, Zhang Y, et al. CD4+ regulatory T cells require CTLA-4 for the maintenance of systemic tolerance [published correction appears in J Exp Med 2009;206:721]. J Exp Med 2009;206:421–34.

Gamradt P, Laoubi L, Nosbaum A, Mutez V, Lenief V, Grande S, et al. Inhibitory checkpoint receptors control $CD8^+$ resident memory T cells to prevent skin allergy. J Allergy Clin Immunol 2019;143:2147–57.e9.

Gebhardt T, Palendira U, Tscharke DC, Bedoui S. Tissue-resident memory T cells in tissue homeostasis, persistent infection, and cancer surveillance. Immunol Rev 2018;283:54–76.

Hasegawa T, Oka T, Son HG, Oliver-García VS, Azin M, Eisenhaure TM, et al. Cytotoxic $CD4^+$ T cells eliminate senescent cells by targeting cytomegalovirus antigen. Cell 2023;186:1417–31.e20.

Hurrell BP, Helou DG, Howard E, Painter JD, Shafiei-Jahani P, Sharpe AH, et al. PD-L2 controls peripherally induced regulatory T cells by maintaining metabolic activity and Foxp3 stability. Nat Commun 2022;13:5118.

Kamenjarin N, Hodapp K, Melchior F, Harms G, Hartmann AK, Bartneck J, et al. Cross-presenting Langerhans cells are required for the early reactivation of resident $CD8^+$ memory T cells in the epidermis. Proc Natl Acad Sci U S A 2023;120:e2219932120.

Kölgen W, Both H, van Weelden H, Guikers KL, Bruijnzeel-Koomen CA, Knol EF, et al. Epidermal langerhans cell depletion after artificial ultraviolet B irradiation of human skin in vivo: apoptosis versus migration. J Invest Dermatol 2002;118:812–7.

Kumar BV, Ma W, Miron M, Granot T, Guyer RS, Carpenter DJ, et al. Human tissue-resident memory T cells are defined by core transcriptional and functional signatures in lymphoid and mucosal sites. Cell Rep 2017;20:2921–34.

Liu X, Zhu R, Luo Y, Wang S, Zhao Y, Qiu Z, et al. Distinct human Langerhans cell subsets orchestrate reciprocal functions and require different developmental regulation. Immunity 2021;54:2305–20.e11.

Lutz MB, Döhler A, Azukizawa H. Revisiting the tolerogenicity of epidermal Langerhans cells. Immunol Cell Biol 2010;88:381–6.

Moorhead JW. Tolerance and contact sensitivity to DNFA in mice. VIII. Identification of distinct T cell subpopulations that mediate in vivo and in vitro manifestations of delayed hypersensitivity. J Immunol 1978;120:137–44.

Nadelmann ER, Yeh JE, Chen ST. Management of cutaneous immune-related adverse events in patients with cancer treated with immune checkpoint inhibitors: a systematic review. JAMA Oncol 2022;8:130–8.

Nakagawa S, Koomen CW, Bos JD, Teunissen MB. Differential modulation of human epidermal Langerhans cell maturation by ultraviolet B radiation. J Immunol 1999;163:5192–200.

Pishesha N, Harmand TJ, Ploegh HL. A guide to antigen processing and presentation. Nat Rev Immunol 2022;22:751–64.

Rambukkana A, Pistoor FH, Bos JD, Kapsenberg ML, Das PK. Effects of contact allergens on human Langerhans cells in skin organ culture: migration, modulation of cell surface molecules, and early expression of interleukin-1 beta protein. Lab Invest 1996;74:422–36.

Rattis FM, Concha M, Dalbiez-Gauthier C, Courtellemont P, Schmitt D, Péguet-Navarro J. Effects of ultraviolet B radiation on human Langerhans cells: functional alteration of CD86 upregulation and induction of apoptotic cell death. J Invest Dermatol 1998;111:373–9.

Rosenblum MD, Gratz IK, Paw JS, Lee K, Marshak-Rothstein A, Abbas AK. Response to self antigen imprints regulatory memory in tissues. Nature 2011;480:538–42.

Ryan GE, Harris JE, Richmond JM. Resident memory T cells in autoimmune skin diseases. Front Immunol 2021;12:652191.

Seneschal J, Clark RA, Gehad A, Baecher-Allan CM, Kupper TS. Human epidermal Langerhans cells maintain immune homeostasis in skin by activating skin resident regulatory T cells. Immunity 2012;36:873–84.

Stoitzner P. The Langerhans cell controversy: are they immunostimulatory or immunoregulatory cells of the skin immune system? Immunol Cell Biol 2010;88:348–50.

Tokura Y, Phadungsaksawasdi P, Kurihara K, Fujiyama T, Honda T. Pathophysiology of skin resident memory T cells. Front Immunol 2020;11:618897.

Watanabe R, Gehad A, Yang C, Scott LL, Teague JE, Schlapbach C, et al. Human skin is protected by four functionally and phenotypically discrete populations of resident and recirculating memory T cells. Sci Transl Med 2015;7:279ra39.

Zhou L, Jiang A, Veenstra J, Ozog DM, Mi QS. The roles of skin Langerhans cells in immune tolerance and cancer immunity. Vaccines (Basel) 2022;10:1380.

This work is licensed under a Creative Commons Attribution-NonCommercial-NoDerivatives 4.0 International License. To view a copy of this license, visit http://creativecommons.org/licenses/by-nc-nd/4.0/